

Characterization of west African shallow flood plains with L- and C-band radar

NICK VAN DE GIESEN

Center for Development Research, Bonn University, Walter-Flex St 3, D-53113 Bonn, Germany
e-mail: nick@uni-bonn.de

Abstract The flood plains along the major rivers of West Africa are a potentially important agricultural resource. Satellite-based radar imagery can be used for characterization of flood patterns. Using dry and wet season Shuttle Imaging Radar (SIR-C) imagery, flood plain elements were classified as gallery-forests, open water, water with reeds, and non-flooded areas. The radar bands used are also available on other satellites (JERS and Radarsat). An error analysis based on histograms shows the results are good despite the lack of real time ground data.

Key words flood plains; multi-frequency analysis; radar; SIR-C; West Africa; wetlands

INTRODUCTION

The west African savanna is crossed by many mid- to large-sized rivers. During the rainy season (May–October), the adjacent flood plains are subject to regular shallow flooding (<100 cm). The flood plains have a high agricultural potential but almost no irrigation development has taken place until now (Marchand, 1987). To ensure an ecologically sound use it is necessary to map and understand the flood dynamics and radar remote sensing can play an important role.

In West Africa, rainy season cloud cover inhibits the use of optical satellite imagery. Radar satellites are not hindered by clouds and are, therefore, the only available instruments for flood characterization. Open water acts like a mirror and scatters almost no microwaves back to the satellite. Flooded areas show up as distinct dark areas, which explains the success of radar for flood mapping (Hess *et al.*, 1995; Pope *et al.*, 1994). Two issues are explicitly addressed: (a) Existing classification schemes are empirical and based on data collected on the ground. Here, the need for ground data is circumvented by looking in greater detail at the backscatter statistics of the landscape. (b) Classification of tropical marshes is typically based on fully polarized radar images from experimental systems (Pope *et al.*, 1997). Here, only data comparable to those from Radarsat (C_{HH}) and JERS (L_{HH}) are used.

SPECTRAL CHARACTERISTICS AND CLASSIFICATION

Four dual-polarized (HH and HV) L- and C-band multi-look-complex images from the April and October 1994 Spaceborne Imaging Radar-C (SIR-C) missions (Stofan *et al.*, 1995) were used. The scenes cover an area in northwest Côte d'Ivoire (9°27'N 7°18'W). Copies are available at <http://edcwww.cr.usgs.gov> under processing numbers 15602/3 and 46351/2. Topographic maps (1:50 000 Odienne 3d and 3b) were used to help delineate the floodplain of the Bâ-Oulé River.

In the April images, a clear boundary can be seen between the smooth and dry plains and the stony and brush-covered uplands (Fig. 1(a)). On-screen digitization, aided by topographic maps, was found to be the most precise way to delineate the flood plains. Approximately one sixth of the plain is occupied by gallery-forests, which show up very brightly. In October, places with shallow or no flooding are covered with reeds, which are bright in C-band. The open water of deeper flooded areas (oxbow lakes) is dark (Fig. 1(c)). Both shallow and deep flooded areas are dark in L-band because reeds do not reflect at this wavelength (Fig. 1(b)). Table 1 gives a quantitative overview of the results.

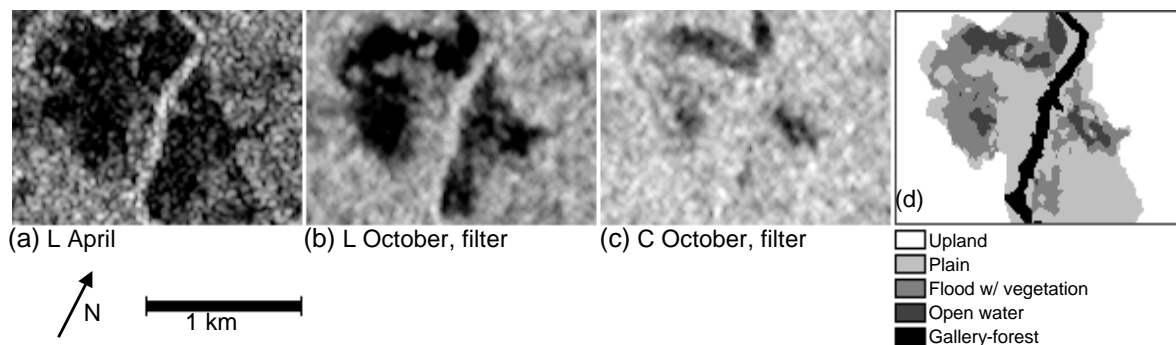


Fig. 1 Detail from Bâ-Oulé flood plain (9°50'N 7°33'W).

Table 1 Mean (SD) backscatter characteristics of flood plain elements in dB.

	Plain	Gallery-forest	Open water	Flood and reeds	Not flooded
L _{HH} April	-19.7 (3.2)	-8.2 (2.9)	na	na	na
C _{HH} April	-15.1 (2.9)	-5.9 (2.8)	na	na	na
L _{HH} October	-15.6 (5.1)	-8.4 (3.3)	-20.4 (5.1)	-20.9 (2.8)	-12.5 (2.6)
C _{HH} October	-8.1 (3.8)	-6.5 (2.9)	-16.3 (2.9)	-10.9 (4.3)	-10.7 (4.1)

L-band backscatter from the flood plain in October has a bi-modal histogram with two peaks representing flooded and non-flooded areas, but with too much variance to make a proper discrimination (Fig. 2). Spatial filters can be used to reduce variance. Hess *et al.* (1995) apply a 5×5 median filter twice before image classification. In our case, this treatment caused too much generalization. Instead, a 5×5 Lee filter, which maintains shapes, was used (Lee, 1981). With reduced variance, open water is distinguishable from vegetated areas in C-band (cutoff at -12.5 dB), and flooded from non-flooded areas in L-band (cutoff at -17 dB). These cut-off values differ from values given elsewhere (Hess *et al.*, 1995; Pope *et al.*, 1994; Pope *et al.*, 1997). The final classification is shown in Fig. 1(d).

ERROR ANALYSIS AND CONCLUSION

Backscatter (σ) from a homogenous area has a Rayleigh probability density function, $\text{pdf}(\sigma) = (\sigma/b^2)\exp(-\sigma^2/2b^2)$, caused by coherent summation of returns from many individual scatterers. Speckle reduction through multi-looking and spatial filtering not

only reduced the variance but also the skewness of the distribution to an extent that a Gaussian pdf applies (Lee, 1981). L-band means for flooded and non-flooded histograms are -20.5 dB and -12.5 dB respectively, and for both $SD = 2.6$ dB. At -17 dB, the histograms intersect. To minimize total error, values below -17 dB were classified as flooded and higher values as non-flooded. On this basis, errors can be calculated (Fig. 2). Of the flooded area, 8.3% was classified as non-flooded and 4.5% of the non-flooded area was classified as flooded. The approach critically relies on the classification being limited to the flood plain and flooded and non-flooded areas having similar sizes.

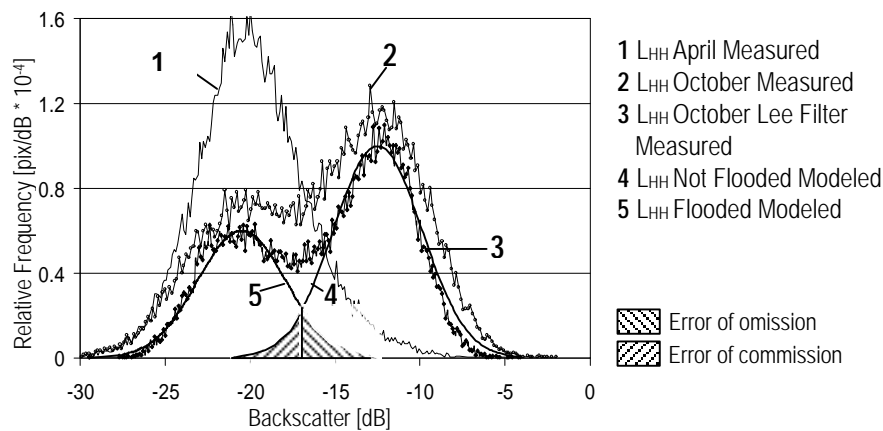


Fig. 2 Histogram analysis of flood plain in October.

The boundary between open water and vegetated flood plain in the C-band is very clear and only 2.1% of the flooded pixels are actually not flooded. This high confidence in the open water delineation provides us with an additional check on the accuracy of the L-band classification. Less than 1% of the open water pixels were classified as not flooded in the L-band, which shows that the -17 dB cut-off value is not too low. It can be concluded that it is indeed possible to map all relevant features of the west African flood plains accurately using only C- and L-band as available on Radarsat and JERS images.

REFERENCES

- Hess, L. L., Melack, J. M., Filoso, S. & Wang, Y. (1995) Delineation of inundated area and vegetation along the Amazon floodplain with the SIR-C Synthetic Aperture Radar. *IEEE Trans. Geosci. Remote Sens.* **33**, 896–903.
- Lee, J.-S. (1981) Speckle analysis and smoothing of synthetic aperture radar images. *Computer Graphics and Image Processing* **17**, 24–32.
- Marchand, R. (1985) The productivity of African floodplains. *Int. J. Environ. Studies* **29**, 201–211.
- Pope, K. O., Rey-Benayas, J. M. & Paris, J. F. (1994) Radar remote sensing of forest and wetland ecosystems in the Central American Tropics. *Remote Sens. Environ.* **48**, 205–219.
- Pope, K. O., Rejmankova, E., Paris, J. F. & Woodruff, R. (1997) Detecting seasonal flooding cycles in marshes of the Yucatan Peninsula with SIR-C polarimetric radar imagery. *Remote Sens. Environ.* **59**, 157–166.
- Stofan, R. E., Evans, D. L., Schmullius, C., Holt, B., Plaut, J. J., van Zyl, J., Wall, S. D. & Way, J. (1995) Overview of results of Spaceborne Imaging Radar-C, X-Band Synthetic Aperture Radar (SIR-C/X-SAR). *IEEE Trans. Geosci. Remote Sens.* **33**, 817–828.